This article was downloaded by: [Renmin University of China]
On: 13 October 2013, At: 10:27
Publisher: Taylor & Francis
Informa Ltd Registered in England and Wales Registered Number: 1072954 Registered office: Mortimer House, 37-41 Mortimer Street, London W1T 3JH, UK

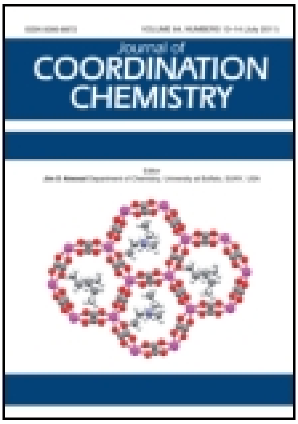

Journal of Coordination Chemistry
Publication details, including instructions for authors and subscription information:
http://www.tandfonline.com/loi/gcoo20

Synthesis, structure, EPR, and DFT calculation on dinuclear paddle wheel Cu(II) complexes with bis-chelate rings

P. Mosae Selvakumar [a], E. Suresh [a], S. Waghmode [b] & P.S. Subramanian [a]

[a] Analytical Science Division, Central Salt and Marine Chemicals Research Institute, Council for Scientific and Industrial Research, Bhavnagar, India

[b] Department of Chemistry, University of Pune, Pune-411 007, India

Published online: 03 Oct 2011.

To cite this article: P. Mosae Selvakumar, E. Suresh, S. Waghmode & P.S. Subramanian (2011) Synthesis, structure, EPR, and DFT calculation on dinuclear paddle wheel Cu(II) complexes with bis-chelate rings, Journal of Coordination Chemistry, 64:20, 3495-3509, DOI: 10.1080/00958972.2011.622754

To link to this article: http://dx.doi.org/10.1080/00958972.2011.622754

PLEASE SCROLL DOWN FOR ARTICLE

Taylor & Francis makes every effort to ensure the accuracy of all the information (the "Content") contained in the publications on our platform. However, Taylor & Francis, our agents, and our licensors make no representations or warranties whatsoever as to the accuracy, completeness, or suitability for any purpose of the Content. Any opinions and views expressed in this publication are the opinions and views of the authors, and are not the views of or endorsed by Taylor & Francis. The accuracy of the Content should not be relied upon and should be independently verified with primary sources of information. Taylor and Francis shall not be liable for any losses, actions, claims, proceedings, demands, costs, expenses, damages, and other liabilities whatsoever or howsoever caused arising directly or indirectly in connection with, in relation to or arising out of the use of the Content.

This article may be used for research, teaching, and private study purposes. Any substantial or systematic reproduction, redistribution, reselling, loan, sub-licensing, systematic supply, or distribution in any form to anyone is expressly forbidden. Terms &

Journal of Coordination Chemistry
Vol. 64, No. 20, 20 October 2011, 3495–3509

Taylor & Francis
Taylor & Francis Group

Synthesis, structure, EPR, and DFT calculation on dinuclear paddle wheel Cu(II) complexes with bis-chelate rings

P. MOSAE SELVAKUMAR†, E. SURESH†, S. WAGHMODE‡
and P.S. SUBRAMANIAN†*

†Analytical Science Division, Central Salt and Marine Chemicals Research Institute,
Council for Scientific and Industrial Research, Bhavnagar, India
‡Department of Chemistry, University of Pune, Pune-411 007, India

(*Received 23 July 2011; in final form 23 August 2011*)

A series of diester-dicarboxylic acids, L^1H_2, L^2H_2, L^3H_2, L^4H_2, and L^5H_2 and their dinuclear Cu_2 complexes $[Cu(L^1)CH_3CN]_2$ (**1**), $[Cu(L^2)H_2O]_2$ (**2**), $[Cu(L^3)CH_3CN]_2$ (**3**), $[Cu(L^4)EtOH]_2$ (**4**), and $[Cu(L^5)CH_3CN]_2$ (**5**), were synthesized. The crystal structures obtained for **1**, **2**, and **4** and the density functional theory optimized structures for **2**, **3**, and **5** illustrated the formation of tetracarboxylate "paddle wheel" complexes. The phthalyl and diphenyl head groups and the spacer moieties were appropriately altered and the size of the chelate ring expanded from 15-membered in **1** to 21-membered in **5**. The dinuclear units have strong Cu–Cu interaction with EPR spectra exploring spin coupled features.

Keywords: Carboxylates; Dinuclear; Paddle wheel complexes; Copper(II); Bis-chelate

1. Introduction

Synthetic host molecules [1] with variable ring size and cavity pertain to molecular recognition [2–4]. Ring compounds such as crown ethers [5], cryptands [6], spherands, and calixarenes [7] play key roles in host–guest chemistry [8]. Cyclic compounds [9–11] possessing metal active sites and macrocyclic rings are potential candidates for functional materials. Metal carboxylates [12] with versatile coordinating capability and ubiquitous presence in many metalloproteins and metalloenzymes inspired the synthesis of dinuclear Cu(II) complexes [13, 14]. Hence, a variety of such metal acetates [14] were synthesized to investigate various aspects such as Cu–Cu interactions, catalysts [15, 16] in many organic reactions, and building blocks in MOF [17]. Monocarboxylic acids with mono, bidentate, chelate, *cis–cis*, *trans–trans*, *cis–trans* coordination modes [18, 19] and *di*- and *polycarboxylic acids* with flexible aliphatic backbones have conformational freedom. Considering the conformational freedom and the diversified coordination provided by carboxylates, we synthesize a series of diester-dicarboxylic acids L^1H_2-L^5H_2. These multidentate ligands, when treated with cupric acetate, form a series of

---

*Corresponding author. Email: siva140@yahoo.co.in; siva@csmcri.org

Journal of Coordination Chemistry
ISSN 0095-8972 print/ISSN 1029-0389 online © 2011 Taylor & Francis
http://dx.doi.org/10.1080/00958972.2011.622754

interesting dinuclear Cu(II) tetracarboxylate complexes, i.e., $[Cu(L^1)CH_3CN]_2$ (**1**), $[Cu(L^2)H_2O]_2$ (**2**), $Cu(L^3)CH_3CN]_2$ (**3**), $[Cu(L^4)EtOH]_2$ (**4**), and $[Cu(L^5)CH_3CN]_2$ (**5**).

McCrindle *et al.* [20, 21] and Bickley *et al.* [22] reported similar bis-chelate complexes, differing by their ether spacer group instead of ester spacer reported in the present complexes. Literature survey shows no such diester-dicarboxylic based paddle wheel Cu_2 complexes except the 15- and 19-membered bis-chelate complexes reported by us [23]. In continuation, this report establishes formation of 15-, 17-, 19-, and 21-membered chelate rings in this series. Complexes **1**–**5** possess chelate rings and Cu(II) active site for potential application in host–guest chemistry and catalysis. Crystal structures obtained for **1**, **2**, and **4** and the density functional theory (DFT) optimized structures of **2**, **3**, and **5** indicate the formation of chelate rings. The strong $Cu\cdots Cu$ interaction and the dinuclear assembly are investigated in detail.

2. Experimental

All chemicals were purchased from Aldrich & Co. Microanalysis of the complexes was done using a Perkin-Elmer PE 2400 series II CHNS/O elemental analyzer. Electronic spectra were recorded on a Shimadzu UV 3101PC spectrophotometer. Mass analyses were performed using electron spray ionization (ESI^+) on a Waters Q Tof-micro mass spectrometer. IR spectra were recorded using KBr pellets on a Perkin-Elmer Spectrum GX FT-IR spectrometer. ^1H and ^{13}C NMR spectra were recorded on a BRUKER *Avance* 200 NMR and 500 NMR spectrometer. The resonance frequencies for ^1H and ^{13}C nuclei were 200.16 and 50.13 (200 MHz) or 500.13 and 125.76 (500 MHz), respectively. ^1H NMR signals were calibrated with respect to TMS, used as an internal reference. Electron spin resonance spectra were recorded using a Bruker X-band Electron Paramagnetic Resonance Spectrometer.

2.1. *Synthesis of ligands*

2.1.1. L^1H_2. The ligand was synthesized following our earlier reported procedure [23].

2.1.2. L^2H_2. 2-({2-[(2-carboxybenzoyl)oxy]-1-methylethoxy}carbonyl) benzoic acid. The above procedure was repeated except using 1,2-propanediol in place of 1,2-ethanediol. Yield 82%. Anal. Calcd (Found) for $C_{19}H_{16}O_8$ (%): C, 61.29(61.08); H, 4.33(4.21). ES-MS: Calcd for $C_{19}H_{16}O_8Na$ $(M+Na)^+$ 395.31; Found: 395.24. ^1H NMR ($CDCl_3$, δ, 500.13 MHz) 8.12–8.53 (b, 2H, OH), 7.827–7.835 (d, 2H, Ar–H), 7.73–7.83 (m, 2H, Ar–H), 7.58–7.591 (d, 2H, Ar–H), 5.49–5.51 (m, 1H, –CH), 4.65–4.68 (q, 1H, $-CH_2$), 4.41–4.43 (q, 1H, $-CH_2$), 1.40–1.42 (d, 3 H, $-CH_3$); $^{13}C[^1H]$ NMR ($CDCl_3$, δ, 125.76 MHz) δ: 173.62 (C=O), 167.33 (C=O), 128.49 (quat –C), 128.58 (quat –C), 129.83 (=CH), 131.37 (=CH), 131.57 (=CH), 70.49 ($-OCH_2$), 67.51 (–OCH), 15.55 ($-CH_2$). IR spectra (ν, cm^{-1}): 3426, 3071, 2966, 2877, 2675, 2542, 1955, 1722, 1694, 1601, 1579, 1493, 1458, 1420, 1311, 1253, 1126, 1076, 1038, 941, 806, 745.

2.1.3. L^3H_2. 2-[({(2Z)-4-[(2-carboxybenzoyl)oxy]but-2-enyl}oxy)carbonyl]benzoic acid. The above-mentioned procedure for L^1H_2 was repeated except using *cis*-but-2-ene-1,4-diol (0.02 mol, 1.645 mL) in place of 1,2-ethanediol. Yield 68%. Anal. Calcd (Found) for $C_{20}H_{16}O_8$ (%): C, 62.50(62.80); H, 4.19(4.30)%. ES-MS: Calcd for $C_{20}H_{16}O_8Na$ $(M+Na)^+$ 407.07; Found: 407.02; ^1H NMR (CD_3OD, δ, 200.16 MHz): 7.65–7.64 (m, ArH, 2H); 7.60–7.56 (m, ArH, 6H) 5.94, 5.92, 5.90 (t, CH, 2H, $J = 4$ Hz) 4.98, 4.96, 4.94 (d, 4H, $-CH_2$). $^{13}C[^1H]$ NMR (CD_3OD, δ, 50.3 MHz); 170.35, 169.68 (C=O), 134.03, 133.28 (quat –C), 132.48, 132.08, 130.26, 129.15 (CH), 129.58 (quat –C), 62.31 ($-OCH_2$). IR spectra (ν, cm^{-1}, KBr): 3359, 2971, 2881, 2676, 2558 (CH str), 1735 (st, int, ν_{COO}); 1687, 1416, 1343, 1281, 1254, 1126 (C–O), 955, 743.

2.1.4. L^4H_2. The ligand was synthesized following our earlier reported procedure [23].

2.1.5. L^5H_2. 2′,2″-(1,2-phenylenebis(methylene))bis(oxy)bis(oxo methylene)dibiphenyl-2-carboxylic acid. The above-mentioned procedure for L^4H_2 was repeated using benzene 1,2-dimethanol in place of 1,2-ethanediol. Yield 78%. Anal. Calcd (Found) for $C_{36}H_{26}O_8$ (%): C, 73.71 (73.45); H, 4.47 (4.42). ESI-MS: Calcd for $C_{36}H_{26}O_8Na$ $(M+Na)^+$ 609.15; Found: 609.26; ^1H NMR (CD_3OD, δ, 500.13 MHz): 7.95–7.93 (d, 2H, Phenyl), 7.78–7.77 (d, 2H, Phenyl), 7.55–7.52 (t, 2H, Phenyl), 7.41–7.369 (quat, 4H, Phenyl), 7.26–7.21 (m, 4H, Phenyl), 7.17–7.15 (d, 2H, Phenyl), 7.07–7.06 (d, 2H, Phenyl), 7.03–7.02 (d, 2H, Phenyl), 4.89 (s, $-CH_2$, 4H). $^{13}C[^1H]$-NMR (CD_3OD, δ, 125.76 MHz): 168.94 (C=O), 167.16 (C=O) 143.33 (quat –C), 143.17 (quat –C), 133.98 (=CH), 131.23 (=CH), 130.89 (=CH), 130.16 (=CH), 1129.91 (=CH), 129.60 (=CH), 128.07 (=CH), 126.74 (=CH), 63.71 ($-CH_2$). IR spectra (ν, cm^{-1}, KBr): 3405, 3062, 2647, 1724 (st, int), 1698, 1444, 1403, 1373, 1286, 1251, 1130, 754.

2.2. *Synthesis of complexes*

2.2.1. $[Cu(L^1)CH_3CN]_2$ (1). Ethanolic solutions of $[Cu(CH_3COO)_2]\cdot H_2O$ (0.398 gm, 0.002 mol) and L^1H_2 (0.716 gm, 0.002 mmol) were mixed and constantly stirred followed by addition of triethylamine (5.5 mL, 0.004 mmol). Transition from green to pale blue was observed indicating complexation. A resultant precipitate was separated, washed with water, and dried. Suitable pale blue single crystals were obtained from acetonitrile-chloroform upon slow evaporation at room temperature for 48 h. Yield 75%. Anal. Calcd (Found) for $C_{40}H_{30}Cu_2O_{16}N_2$ (%): C, 52.12 (52.17); H, 3.28 (3.16); N, 3.04 (2.96). ES-MS: Calcd for $C_{36}H_{24}Cu_2O_{16}Na$ $(M+Na)^+$: 860.96. Found: 861.18. UV-Vis (CH_3CN, λ, nm, ε, $(mol\,L^{-1})^{-1}cm^{-1}$): 269 (1950), 699 (516). IR spectra (ν, cm^{-1}, KBr): 3069, 2967, 2358, 1719, 1631, 1595, 1401, 1283, 1255, 1121, 1082, 838, 753.

2.2.2. $[Cu(L^2)H_2O]_2$ (2). The above procedure for **1** was repeated using L^2H_2 in place of L^1H_2. The complex was crystallized in aqueous ethanol and acetonitrile mixture. Yield 75%. Anal. Calcd (Found) for $C_{38}H_{32}Cu_2O_{18}$ (%): C, 50.50 (50.47); H, 3.57 (3.58). ES-MS: Calcd for $C_{38}H_{28}Cu_2O_{16}$ $(M+H)^+$: 866.00. Found: 867.02. UV-Vis: (CH_3CN, λ, nm, ε, $(mol\,L^{-1})^{-1}cm^{-1}$) 260 (1935), 730 (448). IR spectra (ν, cm^{-1}): 3421, 3072, 2987, 1722, 1633, 1405, 1287, 1254, 1128, 1071, 965, 750.

2.2.3. $[Cu(L^3)CH_3CN]_2$ (3). The procedure for **1** was repeated using L^3H_2 in place of L^1H_2 and **3** was recrystallized in acetonitrile. Yield 70%. Anal. Calcd (Found) for $C4_4H_{36}Cu_2N_2O_{16}$ (%): C, 54.27 (54.48); H, 3.53 (3.66); N, 2.88 (2.83). ES-MS: Calcd for $C_{40}H_{28}Cu_2O_{16}Na$ $(M+Na)^+$: 912.99. Found: 913.16. UV-Vis (CH_3CN, λ, nm, ε, $(mol\,L^{-1})^{-1}cm^{-1}$): 273 (1725), 700 (467). IR spectra (ν, cm^{-1}): 3059, 2356, 1954, 1715, 1627, 1593, 1404, 1283, 1257, 1126, 1077, 1038, 959, 749.

2.2.4. $[Cu(L^4)EtOH]_2$ (4). The procedure for **1** was repeated using L^4H_2 in place of L^1H_2; complex **4** was crystallized in ethanol. Yield 60%. Anal. Calcd (Found) for $C_{64}H_{52}Cu_2O_{18}$ (%): C, 62.18(62.34); H, 4.24(4.26). ES-MS: Calcd for $C_{60}H_{40}Cu_2O_{16}Na$ $(M+Na)^+$: 1165.08. Found: 1165.66. UV-Vis (CH_3CN, λ, nm, ε, $(mol\,L^{-1})^{-1}cm^{-1}$): 315(1255), 699(534). IR spectra (ν, cm^{-1}): 3440, 3060, 2969, 2360, 1944, 1712, 1623, 1596, 1402, 1285, 1252, 1128, 1085, 1048, 848, 756.

2.2.5. $[Cu(L^5)CH_3CN]_2$ (5). The procedure for **1** was repeated using L^5H_2 in place of L^1H_2; complex **5** was recrystallized in acetonitrile. Yield 58%. Anal. Calcd (Found): for $C_{76}H_{54}Cu_2N_2O_{16}$ (%): C, 66.23 (66.11); H, 3.95 (3.86); N, 2.03 (2.13). ES-MS: Calcd for $C_{72}H_{48}Cu_2O_{16}$ $(M+H)^+$: 1294.15. Found: 1296.00. UV-Vis (CH_3CN, λ, nm, ε, $(mol\,L^{-1})^{-1}cm^{-1}$): 318 (1464), 671 (535). IR spectra (ν, cm^{-1}): 3061, 2363, 1946, 1713, 1624, 1596, 1401, 1284, 1253, 1122, 1089, 1045, 933, 753.

2.3. *Crystallography*

Suitable single crystals for **1**, **2**, and **4** were selected under the microscope and immersed immediately in partone oil mounted on the tip of a glass fiber and cemented using epoxy resin. Intensity data for all three crystals were collected using Mo-Kα ($\lambda = 0.71073$ Å) radiation on a Bruker SMART APEX diffractometer equipped with a CCD area detector at 100 K. The data integration and reduction were processed with SAINT [24] software. An empirical absorption correction was applied to the collected reflections with SADABS [25]. The structures were solved by direct methods using SHELXTL [26] and refined on F^2 by full-matrix least-squares using the SHELXL-97 [27] package. Graphics were generated using PLATON [28] and MERCURY 1.3 [29]. In all three complexes, the non-hydrogen atoms were refined anisotropically until convergence. Hydrogen atoms in the ligands were fixed at idealized positions.

2.4. *Modeling*

Computational study of the Cu transition metal complexes has been carried out using DFT [30] methods implemented in Gaussian 03 DFT. The structures studied herein were subjected to unrestricted energy minimizations by using hybrid-DFT B3LYP [31, 32] exchange correlation functional and the double-ζ 6-311+G(d,p) basis set for all atoms in **2** and **3**, whereas double-ζ 6-31+G(d,p) was used for **5**. Normal self-consistent field (SCF) and geometry convergence criteria were employed throughout using either C_S or C_1 symmetry. The calculated geometries with all bond lengths and bond angles are within standard errors expected for geometry optimizations using the B3LYP exchange correlation functional and the 6-31+G(d,p) and 311+G(d,p) basis set. Small differences arise from a combination of inherent errors in DFT calculations and from error associated with comparison of experimental solid-state structures with DFT optimized structures (S7).

3. Results and discussion

Scheme 1 represents the synthesis of diester-dicarboxylic acids and the respective dinuclear Cu(II) complexes. L^1H_2, L^2H_2, and L^3H_2 were obtained by desymmetrizing phthalic anhydride [33, 34] with appropriate diols, such as 1,2-ethanediol, 1,2-propanediol and 1,4-*cis*-butene-diol, respectively. Similarly L^4H_2 and L^5H_2 were obtained upon coupling diphenic head group with 1,2-ethanediol and 1,2-benzenedimethanol spacers, respectively. These ligands possess two carboxylic units at their terminal phenyl and two ester groups in their spacer unit. The synthetic approach with 1 : 1 copper(II)acetate/ligand ratio offered a series of Cu_2 bis-chelate complexes $[Cu(L^1)CH_3CN]_2$ (**1**), $[Cu(L^2)H_2O]_2$ (**2**), $[Cu(L^3)CH_3CN]_2$ (**3**), $[Cu(L^4)EtOH]_2$ (**4**), and $[Cu(L^5)CH_3CN]_2$ (**5**). Mass spectral data (S1) obtained for all these complexes showed the characteristic positive *m*/*z* ion peak and are in accord with formation of dicopper formulae showing an excellent agreement with calculated and experimental values. It may be noted that the mass values of all ligands and complexes correspond to the Na^+ adduct [complex+Na^+] and K^+ adduct [complex+K^+] is well-known [35] in LCMS.

3.1. *Electronic spectra*

UV-Vis electronic spectra (S2) recorded in acetonitrile for these complexes exhibit a broad band at 700 nm attributable to d–d transition. UV band at 270–313 nm may be assigned to ligand to metal charge transition mediated through carboxylate oxygen to Cu(II) and ligand centered transition. The UV-Vis spectra resemble spectra of cupric acetate, confirming similar geometry. The crystal structures determined for **1**, **2**, and **4** with solvent coordination further confirm that axial coordination site for all these complexes are similar to that of cupric acetate. Depending upon the position of the d–d band, the complexes could be arranged in the order of increasing wavelength (λ nm, ε) **5**(671, 535) < **4**(699, 534) ≈ **1**(699, 516) ≈ **3**(700, 467) < **2**(730, 448).

3.2. *IR spectra*

IR spectra for **1**–**5** and L^1H_2–L^5H_2 were recorded in KBr. The diester-dicarboxylic acids had two sets of intense peaks at 1717–1735 cm^{-1} and 1688–1698 cm^{-1} corresponding to ν_{asym} of C=O of the ester and acid, respectively. Intense peaks at 1416–1445 cm^{-1} may be assigned to the ν_{sym} of C=O of terminal COO group. As indicated in table 1, upon complexation with Cu(II) these ligands retained a similar IR pattern with significant shift of the carboxylate. The difference between ν_{asym} and ν_{sym} of COO is a sensitive tool

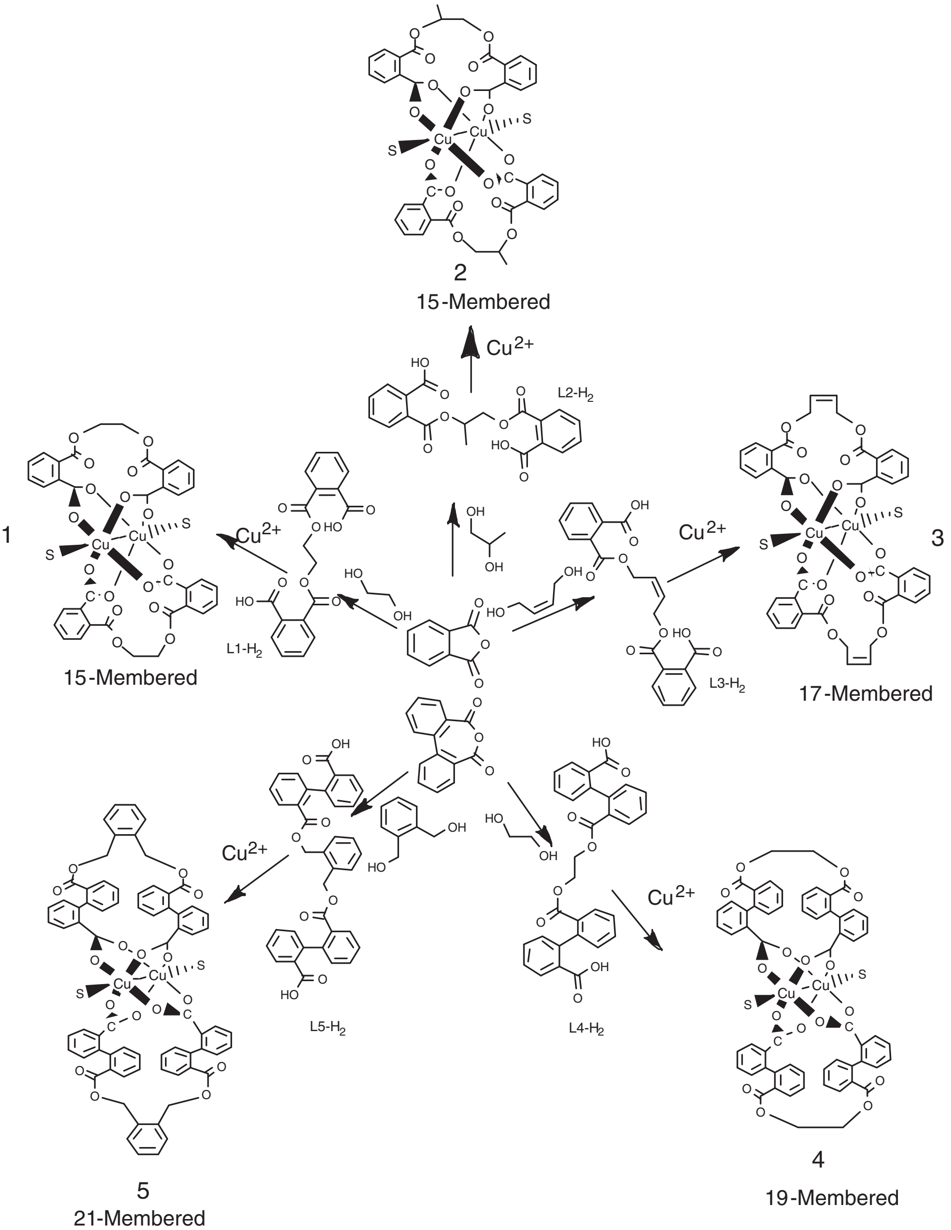

Scheme 1. Schematic representation for the synthesis of ligands and its complexes, where "S" denotes the solvent.

[18, 36] to understand the mode of carboxylate coordination; $\Delta\nu$ falling well in the range 221–230 cm^{-1} indicates *syn–syn* coordination with Cu^{II}. The broad band at 3200–3400 cm^{-1} and a sharp band with medium intensity at 930–955 cm^{-1} of the ligands are attributed to O–H stretching and bending. These bands disappear in their respective Cu(II) complexes, revealing complexation.

Table 1. IR spectral data for ligands and **1–5**.

Compound	Ester ν_{asym} (C=O) cm^{-1}	COO ν_{asym} (C=O) cm^{-1}	COO ν_{sym} (C=O) cm^{-1}	$\Delta\nu = [\nu_{asym} - \nu_{sym}]$ cm^{-1}
L^1H_2	1723	1694	1419	–
L^2H_2	1730	1694	1420	–
L^3H_2	1735	1687	1416	–
L^4H_2	1717	1688	1445	–
L^5H_2	1724	1698	1444	–
1	1719	1631	1401	230
2	1722	1633	1405	228
3	1715	1627	1404	223
4	1712	1623	1402	221
5	1713	1624	1401	223

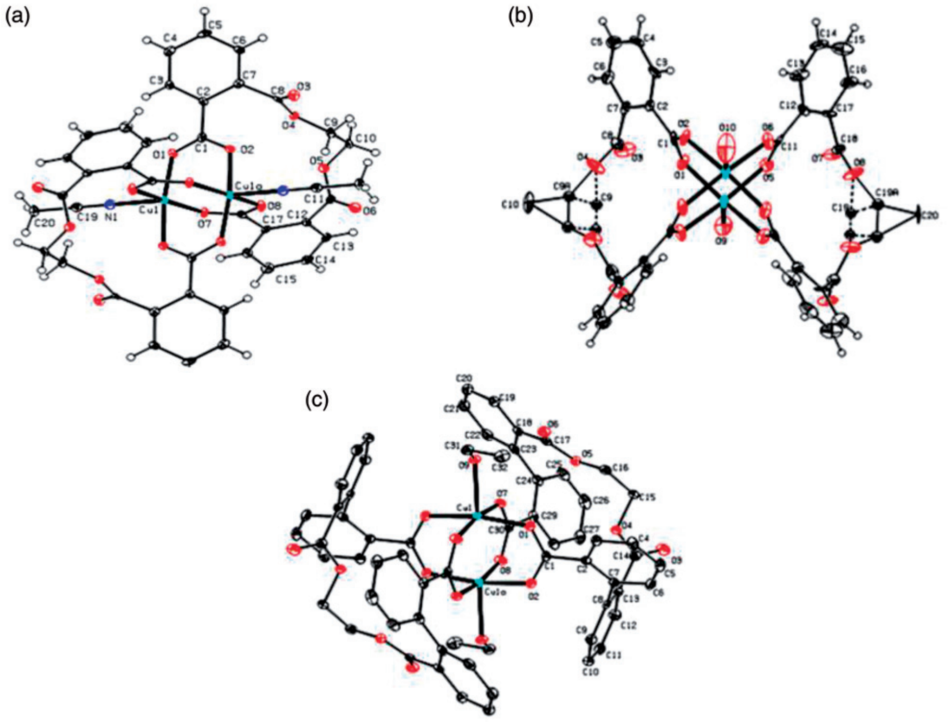

Figure 1. ORTEP diagrams of the complex (a) $[Cu(L^1)CH_3CN]_2$ (**1**), (b) $[Cu(L^2)H_2O]_2$ (**2**) (the lattice CH_3CN molecule is omitted for clarity), and (c) $[Cu(L^4)EtOH]_2$ (**4**) (30% probability factor for all thermal ellipsoids).

3.3. *Structural investigation*

ORTEP diagrams of the dinuclear Cu(II) complexes **1**, **2**, and **4** are depicted in figure 1 and summaries of crystallographic data are presented in table 2. Selected bond distances and angles are given in supplementary material (S5). The crystal structures show

Table 2. Summary of the crystallographic data for **1**, **2**, and **4**.

Complex	**1**	**2**	**4**
Chemical formula	$C_{40}H_{30}Cu_2N_2O_{16}$	$C_{40}H_{19}Cu_2NO_{18}$	$C_{64}H_{50}Cu_2O_{18}$
Formula weight	921.74	928.64	1234.12
Unit cell dimensions (Å, °)			
a	10.1101(11)	21.269(2)	13.3688(15)
b	10.0508(12)	20.381(2)	14.6554(16)
c	19.278(2)	20.644(3)	15.5964(17)
α	90	90	73.123(2)
β	103.262(2)	90	86.871(2)
γ	90	90	78.228(2)
Volume (Å3), Z	1906.6(4), 2	8948.8(18), 8	2862.6(5), 2
Crystal system	Monoclinic	Orthorhombic	Triclinic
Space group	$P2_1/n$	$Cmca$	$P\bar{1}$
Calculated density (g cm^{-3})	1.606	1.379	1.432
Absorption coefficient (mm^{-1})	1.196	1.022	0.818
Temperature (K)	100(2)	100(2) K	100(2)
Final R $(F_o^2)^a$	0.0698	0.1433	0.0810
Weighted R $(F_o^2)^b$	0.1285	0.2939	0.1632
$R_{(int)}$	0.0679	0.1921	0.0381
Residual electron density max/min (e Å^{-3})	0.735 and −0.610	1.310 and −1.366	1.939 and −1.700

$R = \sum|F_o - F_c|/\sum|F_o|$; $Rw = [Sw(F_o^2 - F_c^2)^2]/S[w(F_o^2)^2]^{1/2}$; $w = 1/\sigma(F_o)^2$.

symmetrically disposed deprotonated ligands coordinating through both oxygen atoms of terminal carboxylates in *syn–syn* mode generating a dinuclear Cu(II) "paddle wheel" [37], similar to that of $[Cu(CH_3COO)_2H_2O]_2$. The Cu–Cu distances 2.6248(10) Å in **1**, 2.634(3) Å in **2** and 2.6024 Å [Cu(1)–Cu(1)] in **4a** and 2.5863 Å, [Cu(2)–Cu(2)] in **4b** indicate a strong intermetallic interaction. The phenyl rings C2–C7 and C8–C13 of L^1 are twisted by 83.93°.

3.3.1. Bis-chelate ring.

For L^1H_2–L^3H_2 with phthalyl head groups, the spacer moieties were varied by 1,2-ethanediol, 1,2-propanediol, and 1,4-*cis*-butenediol, respectively; L^4H_2 and L^5H_2 were composed with diphenic head groups and 1,2-ethanediol or 1,2-benzenedimethanol spacers, respectively. Thus the series of ligands possessing different head groups and spacers vary in their length. Upon complexation the ligands establish an interesting macrocycle-like chelate-ring, incorporating Cu(II). Thus **1**, **2**, and **3** possessing phthalyl head group generate 15-membered and 17-membered bis-chelate rings which expand to 19- and 21-membered rings in **4** and **5**. L^2, possessing a chiral centre at its isopropyl spacer, has (*R*) and (*S*) isomers. The racemic mixture might provide racemic Cu(II) complexes; each Cu_2 unit possessing two such ligands can form (*RR*), (*SS*), or (*RS*) pairs. However, isopropyl moiety of L^2 in **2** shows severe disorder preventing assignment of the chirality of the asymmetric carbon. Similarly, **4** with 2,2′-diphenic acid can twist within the diphenic moiety indicating the existence of axial chirality. The phenyl rings C18–C23 and C24–C29 of L^4 twist with an angle 70.49° to each other. The twist angle in **4** is comparatively higher than its acetonitrile counterpart (where the twist angle is 63°–74°) [23]. Complex **4**, showing two different molecules, **4a** and **4b** in the asymmetric unit, existing opposite to each other, can be pronounced as atropisomers. Depending upon the twist between the phenyl rings, the axial chirality on

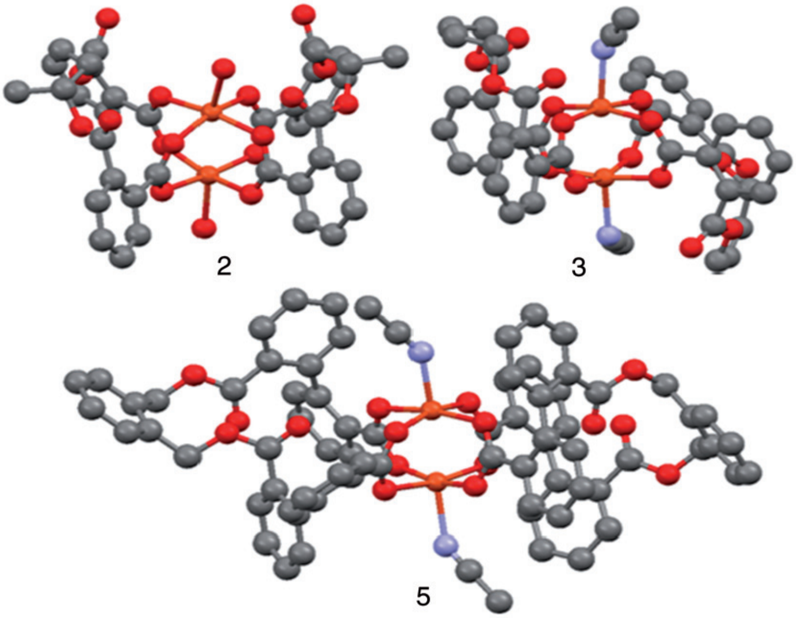

Figure 2. DFT model for **2**, **3**, and **5**.

the C–C axis could be assigned as (*R*)/(*S*) or (*P*)/(*M*) rotation. Each dicopper unit in **4** with four such diphenic moieties has complicated chirality compared to **2** and may generate sixteen different combinations, such as (*RRRR*), (*RSSS*), (*RRSS*), (*SSRR*), (*RRRS*), (*SRRR*), (*SSSR*), (*SSSS*), (*RSRS*), (*SRSR*), (*RSSR*), (*SRRS*), (*RSRR*), (*SRSS*), (*RRSR*), and (*SSRS*). For **4** and **5** with diphenic acid as head group, the twist angle produces interesting atropisomers. Hence these complexes possess chiral properties important in host–guest chemistry and catalysis.

3.4. *Molecular modeling*

Attempts to get single crystals for **3** and **5** failed and hence we optimize the respective structures using DFT along with **2**, which showed severe distortion in its structure. All three optimized structures are shown in figure 2. In addition to the bis-chelate ring, the distances measured for Cu–Cu and Cu–solvent from the experimental and DFT calculations are analyzed below. As observed from the crystal structure and optimized structure the change in the spacer and the number of carbons in expanding the size of the chelate ring does not change the basic paddle wheel geometry. With minor difference in Cu–Cu distances, the flexibility provided by terminal COO and ester COO on the phthalyl facilitate formation of paddle wheel molecules with expanded chelate rings. Similar paddle wheel Cu(II) complexes with acetate and formate bridge reported recently [39, 40] gains significance. Although these molecules do not have bis-chelate rings as in this study, the acetate and formate retained the paddle wheel structure with the shortest Cu–Cu distance, clearly exhibiting flexibility by the spacer moiety facilitates formation of a ‘‘paddle wheel’’.

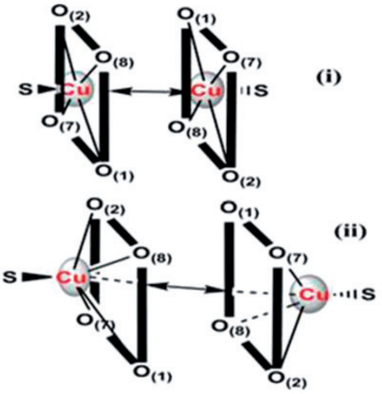

Figure 3. Schematic representation showing the influence of the axially coordinated solvent on the dinuclear Cu(II)–Cu(II) distance. (i) Ideal position of the Cu(II) ion; (ii) Cu(II) ion sitting above the ideal least square plane. Here "S" denotes the solvent.

3.5. *Solvent effect and intermetallic interaction*

As these complexes exist with solvent coordinated, we attempt to derive a correlation between Cu–Cu interaction and solvent coordination. The axial sites in **1**–**5** are found readily replaced by solvent. Complex **1** has acetonitrile [Cu(1)–N(1) = 2.164(4)Å], while complexes **2** and **4** are obtained with water [Cu–O = 2.179(13)–2.124(14) Å] and ethanol [Cu–O = 2.198(3)–2.173(4) Å], respectively, depending upon the solvent in which it was crystallized. Analytical data support the existence of acetonitrile and the Cu–N(CH_3CN) distances are derived from optimized structures of **3** [2.230–2.194 Å] and **5** [2.256–2.182 Å].

Each copper in the dinuclear unit has square-pyramidal geometry with the square base occupied by carboxylate oxygen atoms. The average Cu–O distances in all these complexes are 1.952–1.966 Å. Figure 3 shows the schematic representation of the solvent coordination on the axial site and the subsequent effect in the Cu–Cu distance along with the square formed by the carboxylate oxygen atoms.

Each Cu(II) in **1**, at 0.153 Å above this least squares plane, moved away, lengthening the Cu–Cu distance. Likewise, in **2**, Cu(1) and Cu(2) showed a similar displacement by 0.164 Å from each other, due to stronger coordination with water. The Cu(1) and Cu(2) in **4a** and **4b** were displaced by 0.183 [Cu(1)–Cu(1)] and 0.184 Å [Cu(2)–Cu(2)] above the least squares from strong coordination with ethanol. In the optimized structures of **2**, **3**, and **5**, Cu–Cu distances are 2.639, 2.588, and 2.616 Å, respectively. The change in Cu ⋯ Cu distance is influenced by various factors (table 3), solvent coordination, Cu ⋯ Cu interaction, etc. Based on dinuclear Cu ⋯ Cu distance, the molecules can be arranged as **3** < **4b** < **4a** < **5** < **1** < **2**. Solvent coordination in the axial site plays an important role on the Cu ⋯ Cu interaction, as measured by Cu(II)-solvent distance. The polarity of the solvent significantly influences the intermetallic Cu–Cu distance; water (in **2**) caused longer Cu ⋯ Cu (2.639 Å) distance, indicating migration of Cu(II) in the molecular *z*-direction resulting in weaker intermetallic interaction. Comparatively weak coordinating solvent, acetonitrile, showed medium Cu–Cu distance (S9, S10) in **1**, **3**, and **5**. Depending on Cu–solvent distance, these molecules are arranged

Table 3. Structural data derived from **1** to **5**.

			Crystal data		Simulated	
Complex	Ring size (membered)	Solvent	Cu–Cu	Cu–solvent	Cu–Cu	Cu–solvent
1	15	CH_3CN	2.625	2.165	–	–
2	15	H_2O	2.634	2.123	2.640	2.232
3	17	CH_3CN	–	–	2.619	2.315
4	19	Ethanol	2.602	2.197	–	–
			2.586	2.173	–	–
5	21	CH_3CN	–	–	2.616	2.256

2(2.151) < **1**(2.165) < **3**(2.213) < **5**(2.219) < **4**(2.257 Å). The opposite order shown by Cu–solvent distance and Cu–Cu distance indicates that the axially coordinated solvent significantly affects the intermetallic interaction depending upon its donor strength. Short Cu–Cu distance, 2.58–2.63 Å, inspired us to investigate the copper–copper interaction [41].

EPR spectra recorded for powdered samples of **2** and **3** at room temperature are depicted in figure 4. Electronic spectra of these complexes reveal a similar geometry to Cu(II) acetate [41, 42] and $[Cu(ClCH_2COO)]_2H_2O$. EPR spectra of **2** and **3** also resemble EPR spectra of $Cu(CH_3COO)_2 \cdot 2H_2O$ [43] with zero field splitting (D) significantly greater than $h\nu$ and $E = 0$ (axial symmetry). The spectra are quite incompatible with isolated spins, i.e., $S = 1/2$ for Cu(II), but could be fitted satisfactorily using the interactive spin Hamiltonian for isolated Cu(II) dimers ($S = 1$) as indicated in Equation (1) [43, 44].

$$H = DS_z^2 + E(S_x^2 - S_y^2) + \beta(g_zH_zS_z + g_xH_xS_x + g_yH_yS_y), \tag{1}$$

where D and E are zero field splitting parameters, β is the Bohr magneton, and x, y, z are principle axes, fixed with respect to the $Cu \cdots Cu$ bond. When the external magnetic field is in an arbitrary direction with respect to the x, y, and z axes, we expect in general, three transitions; two $\Delta M_s = \pm 1$ transitions and one $\Delta M_s = \pm 2$ transition. When the magnetic field is along the x, y, and z directions, respectively, one can obtain six $\Delta M_s = \pm 1$ resonance fields from Equation (1) as shown below:

$$\begin{aligned}
H_{x1}^2 &= (g_e/g_x)2[(H_o - D' + E')(H_o + 2E')],\\
H_{x2}^2 &= (g_e/g_x)2[(H_o + D' - E')(H_o - 2E')],\\
H_{y1}^2 &= (g_e/g_y)2[(H_o - D' - E')(H_o - 2E')],\\
H_{y2}^2 &= (g_e/g_y)2[(H_o + D' + E')(H_o + 2E')],\\
H_{z1}^2 &= (g_e/g_z)2[(H_o - D')2 - E'^2)],\\
H_{z2}^2 &= (g_e/g_z)2[(H_o + D')2 - E'^2)],
\end{aligned} \tag{2}$$

where $H_o = h\nu/g_e\beta$, $D' = D/g_e\beta$, and $E' = E/g_e\beta$; H_z^1 and H_z^2 are, for example, the two $\Delta M_S = \pm 1$ transitions when the magnetic field is along the z-axis and g_e is the free electron g-value (2.0023). However, for powder samples, the spectrum is an average of

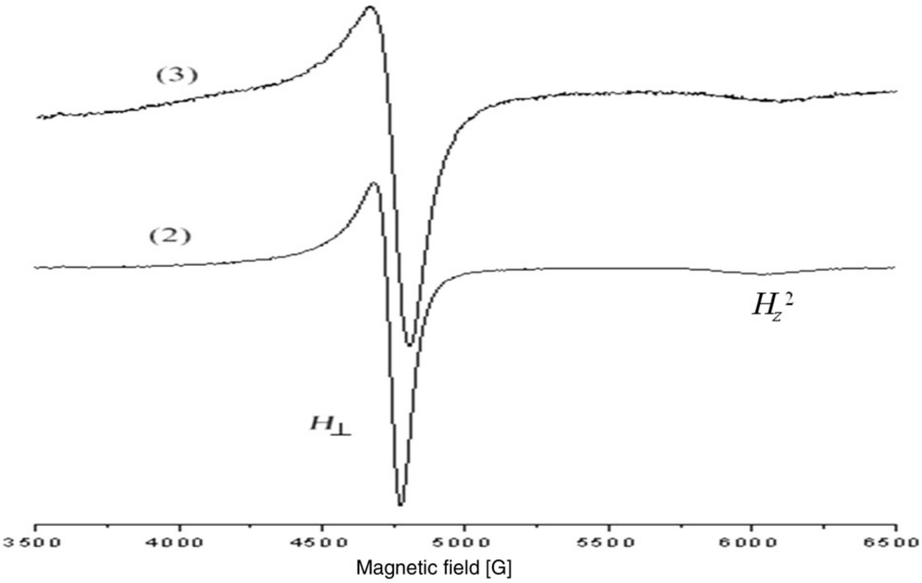

Figure 4. X-band EPR powder spectrum for **2** and **3** at 293 K.

the spectra corresponding to several possible orientations. Six allowed $\Delta M_S = \pm 1$ transitions along with a half-field ($\Delta M_S = \pm 2$) transition are observed for a rhombic symmetry (i.e., $E \neq 0$). When $D < h\nu$, four $\Delta M_S = \pm 1$ transitions along with a half-field ($\Delta M_S = \pm 2$) transition are allowed for axial symmetry ($E = 0$). When $D > h\nu$, as in the case of the present copper dimers at X-band frequency, H_x^1 and H_y^1 and the half-field $\Delta M_S = \pm 2$ transition lines can no longer be observed. Hence the powder spectrum consists of only four lines. If, in addition, $E = 0$, only three EPR lines are observed and Equation (2) can be rewritten as follows:

$$\begin{aligned} H_z^2 &= (g_e/g_z)2[H_o(H_o + D')], \\ H_z^1 &= -(g_e/g_z)(H_o - D'), \\ H_z^2 &= (g_e/g_z)(H_o + D'). \end{aligned} \tag{3}$$

Powdered samples for **2** and **3** show two signals, 4730G and 6100G. In general, the interactive Cu(II) spins, similar to Cu(II) acetate, would give classical triplet state resonance features with three resonances representing H_z^1, $H_\perp$, H_z^2 spin Hamiltonians. The strong signal observed for **2** at 4725 G is attributed to $H_\perp$ and the weak signal at 6040 G representing H_z^2; the signal corresponding to H_z^1 is not observed. Similarly, EPR spectra for **3** exhibit two resonances at 4730 and 6110 G attributable to $H_\perp$ and H_z^2, respectively. Both complexes possess a cage-like Cu_2 and similar paddle wheel Cu_2 acetate structures to cupric acetate and monochlorocupric acetate. EPR spectra reported using X-band for cupric acetate monohydrate and monochlorocupric acetate indicate three resonances including the zero-field resonance at 500–100 G. Complexes **1**–**5** do not show zero-field resonance, suggesting H_z^1 signal falls below 100 G, out of the range of the magnetic field of X-band.

4. Conclusion

We have synthesized a series of Cu_2-tetracarboxylate complexes, which retain the Cu_2 acetate paddle wheel geometry. The bola-shaped diester-dicarboxylic ligands although differing by spacer and head groups form a series of macrocycle-like bis-chelate rings forming *syn-syn* coordination through their terminal carboxylate (COO^-) oxygen atoms with Cu(II). The tetracarboxylate Cu_2 complexes demonstrate expansion of the bis-chelate ring from 15-membered to 21-membered in **1**–**5**. Crystal structures determined for **1**, **2**, and **4** and computational analysis for **2**, **3**, and **5** establish the largest bis-chelate rings reported so far in this series of complexes. Strong intermetallic interactions observed in the dimers was explored using room temperature EPR spectra. Increased ligand strength and the corresponding change in d–d transitions indicate that these complexes can play roles, parallel to the cupric acetate, in catalysis, synthesis, and molecular recognition; work in this direction is in progress.

Supplementary material

The ^{1}H NMR spectra recorded for the ligand, cartesian coordinates determined by the DFT method for **2**, **3**, and **5** are available as supplementary material. Crystallographic data for the structural analysis have been deposited with the Crystallographic Data Center, CCDC Nos 694604 (**1**), 694605 (**2**), and 694606 (**4**). Copies of this information can be obtained free of charge *via* Email: deposit@ccdc.cam.ac.uk or www: http://www.ccdc.cam.ac.uk.

Acknowledgments

We are grateful to Dr D. Srinivas for recording the EPR spectra. This study is supported by Department of Science and Technology New Delhi (India) vide Project Number SR/S1/IC-19/2005. PMSK acknowledges Council for Scientific and Industrial Research (CSIR), India, for Senior Research Fellowship Award.

References

[1] D.J. Cram, J.M. Cram. *Acc. Chem. Res.*, **11**, 8 (1978).
[2] (a) I.O. Sutherland. *Chem. Soc. Rev.*, **15**, 63 (1986); (b) C. Liu, D. Walter, D. Neuhauser, R. Baer. *J. Am. Chem. Soc.*, **125**, 13936 (2003).
[3] J.S. Bradshaw, R.M. Izatt. *Acc. Chem. Res.*, **30**, 338 (1997).
[4] (a) H.S. Chow, E.C. Constable, C.E. Housecroft, M. Neuburger. *Dalton Trans.*, 4568 (2003); (b) C.D. Gutsche. In *Calixarenes: Monographs in Supramolecular Chemistry*, J.F. Stoddart (Ed.), The Royal Society of Chemistry, Cambridge, UK (1989).
[5] C.J. Pedersen. *Angew. Chem. Int. Ed.*, **27**, 1021 (1988). (b) C.J. Pedersen. *J. Am. Chem. Soc.*, **89**, 2495 (1967).
[6] (a) J.-M. Lehn. *Supramolecular Chemistry: Concepts and Perspectives*, VCH, Weinheim (1995); (b) J.-M. Lehn. *Angew. Chem. Int. Ed.*, **27**, 89 (1988).
[7] D.J. Cram. *Angew. Chem. Int. Ed.*, **27**, 1009 (1988).

[8] (a) H.-J. Schneider. *Angew. Chem. Int. Ed.*, **30**, 1417 (1991); (b) R. Kuhn, F. Erni, T. Bereuter, J. Haeusler. *Anal. Chem.*, **64**, 2815 (1992).

[9] (a) M. Fujita, M. Tominaga, A. Hori, B. Therrien. *Acc. Chem. Res.*, **38**, 371 (2005); (b) M. Fujita, J. Yazaki, K. Ogura. *J. Am. Chem. Soc.*, **112**, 5645 (1990); (c) S. Leininger, B. Olenyuk, P.J. Stang. *Chem. Rev.*, **100**, 853 (2000); (d) P.J. Stang, N.E. Persky, J. Manna. *J. Am. Chem. Soc.*, **119**, 4777 (1997); (e) P.H. Dinolfo, J.T. Hupp. *Chem. Mater.*, **13**, 3113 (2001); (f) F.A. Cotton, C. Lin, A. Murillo. *Acc. Chem. Res.*, **34**, 759 (2001); (g) S.-Y. Chang, M.-C. Um, H. Uh, H.-Y. Jang, K.-S. Jeong. *Chem. Commun.*, 2026 (2003).

[10] (a) A.D. Cutland, R.G. Malkani, J.W. Kampf, V.L. Pecoraro. *Angew. Chem. Int. Ed.*, **39**, 2689 (2000); (b) G. Psomas, A.J. Stemmler, C. Dendrinou-Samara, J.J. Bodwin, M. Schneider, M. Alexiou, J.J. Kampf, D.P. Kessissoglou, V.L. Pecoraro. *Inorg. Chem.*, **40**, 1562 (2001); (c) A.D. Cutland, J.A. Halfen, J.W. Kampf, V.L. Pecoraro. *J. Am. Chem. Soc.*, **123**, 6211 (2001); (d) J.J. Bodwin, A.D. Cutland, R.G. Malkani, V.L. Pecoraro. *Coord. Chem. Rev.*, **216-217**, 489 (2001); (e) S.-Y. Yu, Q.-F. Sun, T.K.-M. Lee, E.C.-C. Cheng, Y.-Z. Li, V.W.-W. Yam. *Angew. Chem. Int. Ed.*, **47**, 4551 (2008).

[11] (a) B. Jacques, C. Dro, S. Bellemin-Laponnaz, H. Wadepohl, L.H. Gade. *Angew. Chem. Int. Ed.*, **47**, 4546 (2008); (b) G. Mezei, C.M. Zaleski, V.L. Pecoraro. *Chem. Rev.*, **107**, 4933 (2007); (c) S.J. Lee, W. Lin. *Acc. Chem. Res.*, **41**, 521 (2008).

[12] R.C. Mehrotra, R. Bohra. *Metal Carboxylates*, pp. 17–89, Academic Press, London (1983).

[13] (a) K.G. Strothkamp, S.J. Lippard. *Acc. Chem. Res.*, **15**, 318 (1982); (b) F.A. Cotton, C.A. Murillo. *Eur. J. Inorg. Chem.*, 4209 (2006).

[14] (a) J.L. Wesemann, M.H. Chisholm. *Inorg. Chem.*, **36**, 3258 (1997); (b) M. Rusjan, Z. Chaia, O.E. Piro, D. Guillon, F.D. Cukiernik. *Acta Cryst.*, **B56**, 666 (2000); (c) H. Miyasaka, C.S. Campos-Fernandez, R. Clerac, K.R. Dunbar. *Angew. Chem. Int. Ed.*, **39**, 3831 (2000); (d) D. Lawton, R. Mason. *J. Am. Chem. Soc.*, **87**, 921 (1965); (e) M.R. Churchill, R. Mason. *Nature*, **204**, 777 (1964); (f) P.D. Meester, S.R. Fletcher, A.C. Skapski. *J. Chem. Soc., Dalton Trans.*, 2575 (1973).

[15] P. Ratnasamy, R. Raja, D. Srinivas. *Philos. Trans. R. Soc., A*, **363**, 1001 (2005).

[16] E.S. Sherman, S.R. Chemler, T.B. Tan, O. Gerlits. *Org. Lett.*, **6**, 1573 (2004); (b) C. Arbez-Gindre, V. Berl, J.-P. Lepoittevin. *Steroids*, **68**, 361 (2003).

[17] S.R. Batten, B.F. Hoskins, B. Moubaraki, K.S. Murray, R. Robson. *Chem. Commun.*, 1095 (2000).

[18] (a) M. Melnik. *Coord. Chem. Rev.*, **42**, 259 (1982); (b) M. Kato, Y. Muto. *Coord. Chem. Rev.*, **92**, 45 (1988); (c) P.S. Subramanian, D. Srinivas. *Polyhedron*, **15**, 985 (1996); (d) P.S. Subramanian, P.C. Dave, V.P. Boricha, D. Srinivas. *Polyhedron*, **17**, 443 (1998).

[19] C.N. Rao, S. Natarajan, R. Vaidhyanathan. *Angew. Chem. Int. Ed.*, **43**, 1466 (2004).

[20] G. Ferguson, A.J. McAlees, R. McCrindle, R.J. Restivo, P.J. Roberts. *J. Am. Chem. Soc.*, **99**, 3170 (1977).

[21] R. McCrindle, G. Ferguson, A.J. McAlees, P.J. Roberts. *J. Chem. Soc., Dalton Trans.*, 1406 (1981).

[22] J. Bickley, R.P. Bonar-Law, M.A.B. Martinez, A. Steiner. *Inorg. Chim. Acta*, **357**, 891 (2004).

[23] P.M. Selvakumar, E. Suresh, P.S. Subramanian. *Inorg. Chim. Acta*, **361**, 1503 (2008).

[24] G.M. Sheldrick. *SAINT*, 5th Edn, Siemens Industrial Automation Inc., Madison, WI (1995).

[25] SADABS. *Empirical Absorption Correction Program*, University of Göttingen, Göttingen, Germany (1997).

[26] G.M. Sheldrick. *SHELXTL Reference Manual: Version 5.1*, Bruker AXS, Madison, WI (1997).

[27] G.M. Sheldrick. *SHELXL-97: Program for Crystal Structure Refinement*, University of Göttingen, Göttingen, Germany (1997).

[28] A.L. Spek. *PLATON-97*, University of Utrecht, Utrecht, The Netherlands (1997).

[29] Mercury 1.3 Supplied with Cambridge Structural Database; CCDC: Cambridge, UK, 2003–2004.

[30] W. Koch, M.C.A. Holthausen. *Chemists Guide to Density Functional Theory*, 2nd Edn, Wiley-VCH, Weinheim, Germany (2001).

[31] M.J. Frisch, G.W. Trucks, H.B. Schlegel, G.E. Scuseria, M.A. Robb, J.R. Cheeseman, J.A. Montgomery, T. Vreven Jr, K.N. Kudin, J.C. Burant, J.M. Millam, S.S. Iyengar, J. Tomasi, V. Barone, B. Mennucci, M. Cossi, G. Scalmani, N. Rega, G.A. Petersson, H. Nakatsuji, M. Hada, M. Ehara, K. Toyota, R. Fukuda, J. Hasegawa, M. Ishida, T. Nakajima, Y. Honda, O. Kitao, H. Nakai, M. Klene, X. Li, J.E. Knox, H.P. Hratchian, J.B. Cross, C. Adamo, J. Jaramillo, R. Gomperts, R.E. Stratmann, O. Yazyev, A.J. Austin, R. Cammi, C. Pomelli, J.W. Ochterski, P.Y. Ayala, K. Morokuma, G.A. Voth, P. Salvador, J.J. Dannenberg, V.G. Zakrzewski, S. Dapprich, A.D. Daniels, M.C. Strain, O. Farkas, D.K. Malick, A.D. Rabuck, K. Raghavachari, J.B. Foresman, J.V. Ortiz, Q. Cui, A.G. Baboul, S. Clifford, J. Cioslowski, B.B. Stefanov, G. Liu, A. Liashenko, P. Piskorz, I. Komaromi, R.L. Martin, D.J. Fox, T. Keith, M.A. Al-Laham, C.Y. Peng, A. Nanayakkara, M. Challacombe, P.M.W. Gill, B. Johnson, W. Chen, M.W. Wong, C. Gonzalez, J.A. Pople. *Gaussian 03, Revision C.02*, Gaussian, Inc., Wallingford, CT (2004).

[32] A.D. Becke. *J. Chem. Phys.*, **98**, 5648 (1993).

[33] S. Muthusamy, B. Gnanaprakasam, E. Suresh. *Org. Lett.*, **8**, 1913 (2006).

[34] Y. Chen, P. McDaid, L. Deng. *Chem. Rev.*, **103**, 2965 (2003).

[35] S. Patra, P. Paul. *Dalton Trans.*, 8683 (2009).

[36] G.B. Deacon, R.J. Phillips. *Coord. Chem. Rev.*, **33**, 227 (1980).

[37] (a) B. Kozlevcar, I. Leban, M. Petric, S. Petrcek, O. Roubeau, J. Reedijk, P. Segedin. *Inorg. Chim. Acta*, **357**, 4220 (2004); (b) F.P.W. Agterberg, H.A.J. Provo'Kluit, W.L. Driessen, H. Oevering, W. Buijs, M.T. Lakin, A.L. Spek, J. Reedijk. *Inorg. Chem.*, **36**, 4321 (1997).

[38] (a) E.L. Eliel, S.H. Wilen, L.N. Mander, *Stereochemistry of Organic Compounds*, p. 1142, Wiley & Sons, New York (1994); (b) F. Leroux. *ChemBioChem.*, **5**, 644 (2004); (c) A.G.J. Ligtenbarg, E.K. van den Beuken, A. Meetsma, N. Veldman, W.J.J. Smeets, A.L. Spek, B.L. Feringa. *J. Chem. Soc., Dalton Trans.*, 263 (1998).

[39] M. Barquin, N. Cocera, M.J. Gonzalez Garmendia, L. Larrinaga, E. Pinilla, M.R. Torres. *J. Coord. Chem.*, **63**, 2247 (2010).

[40] M. Barquin, M.J. Gonzalez Garmedia, L. Larrinaga, E. Pinilla, J.M. Seco, M.R. Torres. *J. Coord. Chem.*, **63**, 1652 (2010).

[41] Bertini, D. Gatteschi. *EPR of Exchange Coupled Systems*, Chap. 10, Springer-Verlag, Berlin (1990).

[42] (a) B. Bleaney, K.D. Bowers. *Proc. R. Soc., London*, **A214**, 451 (1952); (b) H. Abe, J. Shimada. *Phys. Rev.*, **90**, 316 (1953).

[43] (a) S. Chavan, D. Srinivas, P. Ratnasamy. *J. Catal.*, **192**, 286 (2000); (b) J.R. Wasson, C.-I. Shyr, C. Trapp. *Inorg. Chem.*, **7**, 469 (1968).

[44] T.D. Smith, J.R. Pilbrow. *Coord. Chem. Rev.*, **13**, 173 (1974).